An Ecological Robustness Oriented Optimal Power Flow for Power Systems' Survivability

Hao Huang*, *Student Member, IEEE,* Zeyu Mao*, *Student Member, IEEE,* Astrid Layton †, Katherine R. Davis, *Senior Member, IEEE**

***Abstract*—Traditional *optimal power flow* (OPF) ensures power systems are operated safely at minimum cost. Recent disasters have highlighted that a focus on minimizing cost can result in a fragile system, such as the immense economic loss and adverse societal impacts after the 2021 Texas Winter Storm. Resilience objectives must also be considered to guide power system operation through unexpected non-ideal conditions. The long-term survivability of ecosystems against various unexpected catastrophes has been quantified by ecologists using the metric R_{ECO}. The metric depends on a system's network structure and energy flows, enabling its application to power systems to investigate the impact of a bio-inspired power system to address resilience needs. This paper formulates an ecological robustness oriented OPF (R_{ECO} OPF) problem to optimize power systems for reliability and survivability under unexpected contingencies. Six power system cases, ranging from 24- to 500-buses are optimized, comparing the reliability and cost of the R_{ECO} OPF with an economics-driven OPF and a security-constrained OPF (SCOPF). The results show the ecologically-inspired method is able to improve the reliability of the power systems with fewer violations and unsolved scenarios during unexpected disturbances. The results also support the potential to use R_{ECO} to control power flow distribution for improved survivability and resilience.**

***Index Terms*—Optimal Power Flow, Power System Reliability, Power System Resilience, Ecosystems**

[1]

I. Introduction

Power systems are critical infrastructure that deliver electric energy over long distances to support daily life. Their operation requires careful consideration of both the environment and economics, for which there are optimal power flow analysis approaches that consider each individually. The economic-driven optimal power flow (OPF) [1] minimizes operational costs while meeting reliability requirements. The security-constrained optimal power flow (SCOPF) has been used to ensure the safety of power systems with postulate contingencies while minimizing operational costs [2]. SCOPF focuses on *specific* contingencies, so unexpected contingencies can still cause system stress and a loss of load. The 2021 Texas Winter Energy Crisis [3] caused large-scale blackouts due to unexpected extreme weather, leading to generator unavailability. A 2017 grid resilience report by the US National Academies calls for enhanced power system abilities to prepare for, endure, and recover from severe hazards [4]. Hazards of the scale and type to impact the grid are becoming more common, posing a critical question: can existing economics-driven power system operation support survival under unexpected extreme disturbances?

Resilience is a property of systems that describes their ability to operate during and recover from adverse situations to resume normal operations. Resilience depends on the system's elements, configuration, interactions with the surrounding environment, and threats [5]. Resilience metrics based on a multi-phase resilience trapezoid for power system operational and infrastructure resilience [6] and sequential Monte-Carlo-based time-series simulation models to assess power system resilience [7] have been used to help quantify this characteristic. Another availability-based engineering resilience metric uses a dynamic Bayesian network evaluation methodology [8]. These metrics proactively quantify power system resilience under specific threats with historical data and suggest corresponding enhancement methods. While they do provide guidance, they are not sufficient to support power system operations for survivability under unexpected contingencies.

SCOPF is an essential function in power system operation that calculates a secure operating state where *demand is met without reliability violations* in either the base case or under a set of postulated contingencies. The SCOPF problem can be modeled as a mixed-integer nonlinear problem, where predefined contingencies can integrate with the OPF problem through discrete variables [9]. The system size and number of contingencies makes the SCOPF problem nontrivial [2] and so a DC SCOPF model can help improve the efficiency of iterative AC SCOPF algorithms [10]. Approaches to obtain SCOPF solutions under conflicting contingencies are proposed in [11]. Consideration of corrective actions within the SCOPF problem have also been proposed [12], including voltage and frequency control to deal with transients during contingencies [13]. Although SCOPF can efficiently and effectively deal with postulated contingencies, the conventional SCOPF only considers *N-1* contingencies. Unexpected contingencies and those where multiple elements malfunction are not considered and still threaten the security of power system operation.

Several resilience-oriented preventive approaches against extreme weather events have been studied by considering the stochastic nature and fragility curve of power system elements. In [14], it proposes a resilience-oriented hourly unit commitment. In [15], Wang *et al.* present a resilience-constraint economic power dispatch. Both methods aims to improve power system resilience from the economic perspective. Trakas *et al.* formulate a tri-level optimization problem to economically dispatch power flow against the worst scenario from the extreme weather [16]. Zhao *et al.* formulate a two-

This article has been accepted for publication in a future issue of this journal, but has not been fully edited. Content may change prior to final publication. Citation information: DOI 10.1109/TPWRS.2022.3168226, IEEE Transactions on Power Systems

stage distributionally robust and robust optimization problem to mitigate the adverse impact of the worst load forecasting and line failure scenario for day-ahead market [17]. Several robustness-oriented methods are also proposed for power system operations considering cascading failures from cyber and physical adversaries [18]–[21]. An entropy-based robustness metric is proposed in [18] to predict the cascading failures in power systems based on the network topology and power flow distribution. Xiang *et al.* extend the traditional SCOPF considering attacks in power systems, which improves the system's robustness with less loss of load under attacks [19]. Lai *et al.* propose a robustness-oriented economic dispatch model for battery management systems to improve the energy supply in microgrids under attacks [20]. Lai *et al.* also propose both deterministic and stochastic coupling strategies for cyber-physical power systems to improve its robustness against cyber attacks [21]. Various specialized remedial actions against specific events have been developed and employed by utilities to ensure power systems' safety and security after the adverse events [22]. For example, corrective action schemes to provide countermeasures against unexpected contingencies as fast as possible [23], [24].

Line outage distribution factors (LODFs) and group betweenness and centrality (GBC) were used to identify critical contingencies consisting of high-impact sets of multiple elements throughout the system [25], [26]. Such elements widely spread across the system making such contingencies statistically *unexpected* and *adversely stress* the system operation. These contingencies are treated as *unexpected contingencies* in the paper. The failure of such elements, e.g., from extreme weather or other threats as in [27], creates severe impact with violating operating limits. These unexpected contingencies can help approximate high-impact low-frequency (HILF) events. HILF events can be used to help measure the resilience of the power systems by analyzing how resilient the system is under all HILF events. HILF events are not traditionally considered in SCOPF, and stochastic based approaches [14]–[17] only consider the worst scenario from particular HILF events. Thus, there is a research gap of how to operate power systems so that they can survive from unexpected contingencies for long-term resilience. This manuscript presents a novel approach based on long-term resilient ecosystems to fill this research gap.

Ecosystems have evolved to be very good at surviving a wide variety of unexpected catastrophes, demonstrating both their resilience and sustainability. Focusing on energy transfers among species in an ecosystem (a food web model), ecologists have quantitatively connected survivability to network structural and functional characteristics [28]–[30]. Previous work [31]–[34] has translated ecosystem resilience (the ecological robustness metric R_{ECO}), to power systems by using R_{ECO} to guide the design of network structure with improved reliability and resilience. The formulation of R_{ECO} in power systems depends on both the network structure and its power flows. The optimized network structures were able to improve R_{ECO}, measured by their ability to absorb unexpected contingencies with fewer (and often no) violations. R_{ECO} is an information theory-based metric calculated from a steady-state directional graph of a network [28]–[30]. The metric quantifies a balance between pathway *efficiency* (effectiveness when energy is transferred from one node to another) and *redundancy* (energy has multiple pathway options to get from one node to another). Ecosystem have been found to occupy a narrow range of R_{ECO} values, representing a unique balance of these two measures, that suggests the window representing a evolutionarily-superior network design. An ecological robustness oriented optimal power flow (R_{ECO} OPF) problem is presented here to optimize R_{ECO} for a given power system, guiding the power flow dispatch for survivability and reliability.

Surviability is taken here to represent the resilience of power systems. Resilience and survivability are both terms used to describe the system's ability to withstand disturbances, however resilience is commonly demonstrated using a time-series assessment [6] that depends on operation and response strategies against disturbances at different stages. Survivability is measured as how a power system can immediately tolerate or absorb adverse impact when a disturbance happens. Survivability is here treated as the preventative stage in resilience. *Reliability* is one aspect of resilience that is well-known and quantifiable; it is used here to help measure resilience and surviability improvements when disturbances adversely impact the system's operating status. The inherent ability of the power system to absorb disturbances is quantified by R_{ECO}, where a better R_{ECO} means that the system has an increased ability to absorb disturbances for better survivability and resilience.

The main contributions are as follows:

- In this paper, we introduce a new resilience metric for power systems operation, R_{ECO}, to support their survival through unexpected contingencies. An OPF problem to optimize R_{ECO} for its operation (R_{ECO} OPF) is formulated and solved. The optimized cases are validated to test for any improvement in their inherent ability to absorb disturbances without human intervention.
- The feasibility and effectiveness of the proposed R_{ECO} OPF problem is investigated using six power system case studies, ranging from 24- to 500-buses. The cases are solved using Direct Current (DC), Quadratic-Convex relaxed Alternating Current (QCLS), and Alternating Current (AC) power flow models. The achieved optimal R_{ECO} varies under the different power flow models, but it is observed that higher R_{ECO} systems are more resilient against unexpected contingencies.
- Reliability improvements stemming from the R_{ECO} OPF are illustrated using a set of unexpected contingencies and compared to the tradition OPF and SCOPF for resilience improvements and cost-effectiveness. The results support the potential for using R_{ECO} OPF as a preventative method against unexpected contingencies.
- Analyses of network properties regarding the robustness and distribution of power flows show that the power flows in the R_{ECO} optimized cases are more homogeneously distributed, contributing to the measured improvement against cascading failures.

Section II reviews the background of R_{ECO} with respect to power systems and presents the proposed R_{ECO} OPF. Section III introduces the relaxation of R_{ECO} using a Taylor Series

This article has been accepted for publication in a future issue of this journal, but has not been fully edited. Content may change prior to final publication. Citation information: DOI 10.1109/TPWRS.2022.3168226, IEEE Transactions on Power Systems

Expansion and DC & Quadratic-Convex relaxed AC power flow models. Section IV solves the relaxed R_{ECO} OPF for six power system case studies ranging from 24- to 500-buses with different power flow models. Section V evaluates the R_{ECO} OPF to understand improvements in the bio-inspired network's reliability, cost-effectiveness, and other network properties. Discussion of the various results can be found in Section VI.

II. Ecological Robustness Oriented Optimal Power Flow

A. Overview of Ecological Robustness in Power Systems

The input for calculating R_{ECO} is the **Ecological Flow Matrix** [**T**], which is a square $(N{+}3) \times (N{+}3)$ matrix. The N is the number of actors, and the extra entries represent the system inputs, useful outputs, and dissipation [35]. For power systems, we model generators and buses as *actors* whose function is transferring energy in the network, *system inputs* are the energy generated from generators, *useful exports* are the load (consumption), and *dissipation* is the power losses [31]–[34]. The entries in [**T**] are T_{ij}, representing the directed power flow from node i to node j. Fig. 1 shows the constitution of [**T**] for power systems with real power flows. The system inputs are power from generators P_{gen_i}. The useful exports are the loads at each bus, P_{load_i}. Dissipation is P_{loss_i} is the real power loss at Bus i. The generators are treated as lossless, so the dissipation column for generators is 0. The *transitions* are P_{ij} and P_{gen_i}, the power flows of the corresponding branch and between the corresponding bus and generator, respectively. If there is no interaction among buses and generators, the entry is zero.

		Gen 1	. . .	Gen n	Bus 1	. . .	Bus m	Output	Dissipation
Input	0	P_{gen1}	. . .	P_{genn}	0	. . .	0	0	0
Gen 1	0	0	. . .	0	P_{gen1}	. . .	0	0	0
.	.	.	. . .	.	.	. . .	.	.	.
Gen n	0	0	. . .	0	0	. . .	P_{genn}	0	0
Bus 1	0	0	. . .	0	0	. . .	P_{1m}	$P_{load\ 1}$	$P_{loss\ 1}$
.	.	.	. . .	.	P_{i1}	. . .	.	.	.
.	.	.	. . .	.	.	P_{ij}	P_{im}	.	.
Bus m	0	0	. . .	0	P_{m1}	. . .	0	$P_{load\ m}$	$P_{loss\ m}$
	0	0	. . .	0	0	. . .	0	0	0
	0	0	. . .	0	0	. . .	0	0	0

Fig. 1: An *Ecological Flow Matrix* [**T**] for a grid with *n* generators and *m* buses and grid customers residing outside the system boundaries (modeled as useful outputs): The P_{gen_i} is the real power output from generator i, which locates at the input row and the flow between generator and corresponding bus. The generators are treated as lossless, so the dissipation column for generators is 0. The P_{load_i} is the real power consumption at Bus i. P_{loss_i} is the real power loss at Bus i. The P_{ij} is the real power flows at the corresponding branch. If there is no power flow interaction among buses and generators, the entry is zero.

The quantification of R_{ECO} derives from an information theoretic approach considering energy transitions among all species over the network through a model of **surprisal** [28]–[30]. The formulation of R_{ECO} represents robustness as a function of pathway *redundancy* and *efficiency*, shown in ecosystems to be directly related to the long-term survival of the network [30]. **Surprisal** is similar to "information" as defined by Shannon and "entropy" as defined by Boltzmann [36], with the following expression,

$$s = -k \times log(p) \tag{1}$$

where s is one's "surprisal" at observing an event that occurs with probability p, and k is a positive scalar constant.

Using surprisal, the **indeterminacy** of an event i can be described as the product of the presence of an event p_i and its absence s_i:

$$h_i = -k \times p_i \times log(p_i) \tag{2}$$

where h_i is the indeterminacy of the event i.

The indeterminacy measures the potential for change with respect to an event i, where event i must both be likely enough to occur ($p_i >> 0$) and unlikely enough, such that the system is doing something else most of the time ($s_i >> 0$). The interpretation is as follows: for a given system, certain low probability events have a high potential for change or high impact to the system, but they happen rarely; high probability events possess a low impact because they occur often and the system adapts [37].

With surprisal and indeterminacy, R_{ECO} is able to quantify the ecosystem robustness considering prospective events (disturbances) in the system, with following metrics.

The **Total System Throughput** (*TSTp*) [30] is the sum of all flows in [**T**], capturing the system size:

$$TSTp = \sum_{i=1}^{N+3} \sum_{j=1}^{N+3} T_{ij} \tag{3}$$

For power systems, it is the total energy circulated in the system.

The **Ascendency** (*ASC*) measures the scaled mutual constraint for system size and flow organization that describes the process of ecosystems' growth and development [38] with Equation (4):

$$ASC = -TSTp \sum_{i=1}^{N+3} \sum_{j=1}^{N+3} \left(\frac{T_{ij}}{TSTp} log_2 \left(\frac{T_{ij} TSTp}{T_i T_j} \right) \right) \tag{4}$$

where T_i is the $\sum_{j=1}^{N+3} T_{ij}$.

The part of $\sum_{i=1}^{N+3} \sum_{j=1}^{N+3} \frac{T_{ij}}{TSTp} log_2(\frac{T_{ij} TSTp}{T_i T_j})$ is the *average mutual information* introduced in [38], [39], which is the average amount of uncertainty based on the knowledge of food web structure. The food webs include the food chains in a graphical representation among different species in ecosystems based on their prey-predator relationships. The graph captures the flow of energy and materials in ecosystems [40]. The $\frac{T_{ij} TSTp}{T_i T_j}$ considers the knowledge of source (*i*) and end (*j*) nodes for a given flow (*ij*) in the network. Following the indeterminacy in Equation (2), the average mutual information represents the aggregate amount of uncertainty accompanying

This article has been accepted for publication in a future issue of this journal, but has not been fully edited. Content may change prior to final publication. Citation information: DOI 10.1109/TPWRS.2022.3168226, IEEE Transactions on Power Systems

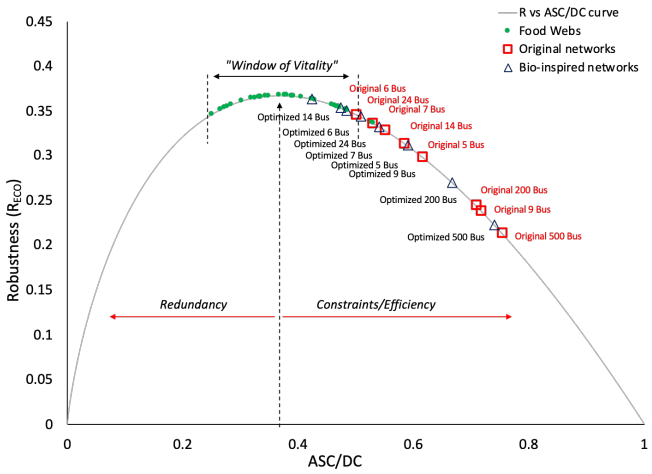

Fig. 2: The ecological robustness curve depicting the eight grids and their bio-inspired optimized versions, as well as a set of 38 food webs. Replicated from [32], [34]

each flow in the system with the knowledge of source and end nodes. Multiplying with *TSTp*, *ASC* gives a dimensional version of network uncertainty. A higher *ASC* for the same size system represents a network that has fewer options of pathways for flows moving from any one actor to another, resulting in a network with a lower level of uncertainty.

The **Development Capacity** (*DC*) was introduced by Ulanowlcz in [41] as the upper bound of *ASC* since there is a limit of ecosystems' growth and development:

$$DC = -TSTp \sum_{i=1}^{N+3} \sum_{j=1}^{N+3} \left(\frac{T_{ij}}{TSTp} log_2 \left(\frac{T_{ij}}{TSTp} \right) \right) \tag{5}$$

where the $\frac{T_{ij}}{TSTp}$ can be recognized as the probability of an event respect to the flows in the system. Let $H_{ij} = \frac{T_{ij}}{TSTp} log_2(\frac{T_{ij}}{TSTp})$ with (2), and *DC* can be rewritten as

$$DC = -TSTp \times \sum_{i=1}^{N+3} \sum_{j=1}^{N+3} H_{ij} \tag{6}$$

Then, a system's *DC* is its aggregate *indeterminacy* that describes its capacity to undergo change. It captures the aggregated impacts (uncertainty) from all events (surprisals).

With the above formulation, the ratio of *ASC* and *DC* reflects the *pathway efficiency* for a given network while its natural logarithm shows the network's *pathway redundancy* [30]. With the power flows as input, the *pathway efficiency* and *redundancy* in power systems consider both the network structure and the amount of power flow distributed over the network. Then, the formulation of R_{ECO} is as follows,

$$R_{ECO} = -\left(\frac{ASC}{DC} \right) ln \left(\frac{ASC}{DC} \right) \tag{7}$$

where R_{ECO} has the ability to account for the presence of unknown events, or interruptions, that can happen in the system.

Fig. 2 shows the comparison of R_{ECO} among food webs, original power networks, and bio-optimized power networks from [31]–[34]. The *ASC/DC* is the ratio of ascendancy and development capacity for a given ecosystem, representing the system's efficiency and redundancy. The R_{ECO} value of robust food webs has been shown to fall into a specific range respect to *ASC/DC*, called the *Window of Vitality*, that circumscribes sustainable behavior in ecosystems [30]. It reflects the beneficial balance of the food webs' efficiency and redundancy of the network structure and energy flows for its survivability.

The calculation of R_{ECO} in power systems depends on both the network structure and its power flows. Thus, the R_{ECO} OPF is proposed to improve power system's robustness for better reliability and survivability against unexpected contingencies by optimizing its power flow distribution.

B. Ecological Robustness Oriented Optimal Power Flow

The proposed R_{ECO} OPF problem is formulated through Equation (8)-(22) under the assumptions of an AC power flow model. Its objective is to maximize the R_{ECO} of a given power system through adjusting the control variables of real (P_i) and reactive power (Q_i) injections, and bus voltages (magnitude V_i and angle θ_i). The problem uses R_{ECO} as the objective, to improve power system robustness for more resilient operation, with better reliability and survivability against disturbances.

Equation (9) is a function of real power flows, including generator real power outputs P_{gen_i}, real power flows P_{ij} in the network, power consumptions at each load P_{load_i}, and power losses P_{loss_i} at each bus; these formulate [**T**] as in Fig. 1. Then, Equations (10)-(13) formulate R_{ECO}, *ASC*, *DC*, and *TSTp*, respectively. Equations (14) - (21) ensure satisfaction of power balance and power system operation constraints with AC power flow model for real and reactive power. We aggregate the branch losses for each bus as P_{loss_i}, with Equation (22),

$$\text{Maximize } (R_{ECO}) \tag{8}$$

subject to:

$$\mathbf{T} = f(P_{ij}, P_{gen_i}, P_{load_i}, P_{loss_i}) \tag{9}$$

$$R_{ECO} = -\left(\frac{ASC}{DC} \right) ln \left(\frac{ASC}{DC} \right) \tag{10}$$

$$ASC = -TSTp \sum_{i=1}^{N+3} \sum_{j=1}^{N+3} \left(\frac{T_{ij}}{TSTp} log_2 \left(\frac{T_{ij} TSTp}{T_i T_j} \right) \right) \tag{11}$$

$$DC = -TSTp \sum_{i=1}^{N+3} \sum_{j=1}^{N+3} \left(\frac{T_{ij}}{TSTp} log_2 \left(\frac{T_{ij}}{TSTp} \right) \right) \tag{12}$$

$$TSTp = \sum_{i=1}^{N+3} \sum_{j=1}^{N+3} T_{ij} \tag{13}$$

$$v_i^l \leqslant V_i \leqslant v_i^u \ (\forall i \in \mathcal{M}) \tag{14}$$

$$s_{ij}^l \leqslant S_{ij} \leqslant s_{ij}^u \ (\forall (i,j) \in \mathcal{B}) \tag{15}$$

This article has been accepted for publication in a future issue of this journal, but has not been fully edited. Content may change prior to final publication. Citation information: DOI 10.1109/TPWRS.2022.3168226, IEEE Transactions on Power Systems

$$s^l_{gen_i} \leqslant S_{gen_i} \leqslant s^u_{gen_i} \ (\forall i \in \mathcal{G}) \tag{16}$$

$$S = P + iQ \tag{17}$$

$$P_{ij} = V_i^2[-G_{ij}] + V_iV_j[G_{ij}cos(\theta_{ij}) + B_{ij}sin(\theta_{ij})] \quad (\forall (i,j) \in \mathcal{B}) \tag{18}$$

$$Q_{ij} = V_i^2[B_{ij}] + V_iV_j[G_{ij}sin(\theta_{ij}) - B_{ij}cos(\theta_{ij})] \quad (\forall (i,j) \in \mathcal{B}) \tag{19}$$

$$P_i = P_{load_i} - P_{gen_i} = \sum_j P_{ij} \ (\forall j \in \mathcal{M}) \tag{20}$$

$$Q_i = Q_{load_i} - Q_{gen_i} = \sum_j Q_{ij} \ (\forall j \in \mathcal{M}) \tag{21}$$

$$P_{loss_i} = \frac{1}{2}\sum_j (P_{ij}^2 + Q_{ij}^2)/(B_{ij}V_i^2) \ (\forall j \in \mathcal{M}) \tag{22}$$

where $\mathcal{B}$, $\mathcal{M}$, and $\mathcal{G}$ are the sets of all branches, buses, and generators; v_i^l and v_i^u are the lower and upper bound of bus voltage magnitude; s_{ij}^l and s_{ij}^u are the lower and upper bound of branch limit; $s^l_{gen_i}$ and $s^u_{gen_i}$ are the lower and upper bound of generator output, respectively.

III. Relaxations for Proposed R_{ECO} OPF

The R_{ECO} OPF problem in `PowerModels.jl` [42] is built here using `Julia` [43]. The formulation of R_{ECO} with Equation (10) - (13) uses power flows at each element based on their network index. The formulation contains the natural logarithm function, whose domain should be positive; its use would require flow directions of P_{gen_i}, P_{load_i}, P_{ij}, and P_{loss_i} to be fixed. However, the flow directions of all P_{ij} depend on V_i, θ_i, P_{gen_i}, and Q_{gen_i}; hence, during the optimization process, they can reverse. Moreover, the logarithm function is a log-concave function [44], which makes the proposed R_{ECO} OPF challenging to solve. The logarithm function's Taylor Series Expansion is first performed to relax the formulation of R_{ECO}. Then, two relaxed schemes of power flow are considered using both a linearized DC power flow model and a Qudratic-Convex relaxed AC power flow model to solve the proposed R_{ECO} OPF problem.

A. Relaxation of R_{ECO} Formulation

There are several Taylor Series Expansions for the natural logarithm function. Considering the domain for the expansion, this paper utilizes the following relaxation with $x > 0$ [45]:

$$\begin{aligned} ln(x) &= 2\sum_{n=1}^{\infty} \frac{((x-1)/(x+1))^{(2n-1)}}{(2n-1)} \\ &= 2[\frac{(x-1)}{(x+1)} + \frac{1}{3}(\frac{(x-1)}{(x+1)})^3 + \frac{1}{5}(\frac{(x-1)}{(x+1)})^5 + ...] \end{aligned} \tag{23}$$

For Equation (5) and (4), the logarithm function is with base of 2. With the property of logarithm function:

$$log_2(x) = \frac{ln(x)}{ln(2)} \tag{24}$$

the Taylor Series Expansion of $log_2(x)$ can be expanded as:

$$log_2(x) = \frac{2}{ln(2)}[\frac{(x-1)}{(x+1)} + \frac{1}{3}(\frac{(x-1)}{(x+1)})^3 + \frac{1}{5}(\frac{(x-1)}{(x+1)})^5 + ...] \tag{25}$$

The above relaxation requires the input x not equal to -1. From Equations (10)-(12), the inputs for the logarithm function are $\frac{ASC}{DC}$, $\frac{T_{ij}TSTp}{T_iT_j}$, and $\frac{T_{ij}}{TSTp}$, respectively. The T_{ij} are power flows in the system. From Fig. 2, the $\frac{ASC}{DC}$ is always bounded within (0,1). Through Equation (11) and (12), $\frac{T_{ij}TSTp}{T_iT_j}$ should be within (0,1). Since the power flow will change direction, $\frac{T_{ij}TSTp}{T_iT_j}$ is bounded within (-1,1). With Equation (13), $\frac{T_{ij}}{TSTp}$ is also bounded within (-1,1) since T_{ij} is always less than $TSTp$. One extreme situation is when the system has only one actor that exports and intakes energy, where the above boundary will include ± 1. However, that is impractical for power systems.

The formulation of R_{ECO} is based on the initial state. By adapting the first order Taylor Series Expansion of Equation (23) and (25) into Equation (10) - (12), so that it can take negative values without logarithm domain restriction during the solving process. A more strict formulation of R_{ECO} that needs to dynamically update during solving process would increase the complexity of the problem and thus adversely affect scalability to large and realistic systems, like the limitation encountered in [32].

B. Approximation of AC Power Flow Models

1) DC Power Flow Model: The basic linearized DC power flow model treats the system as lossless with $\boldsymbol{G} = \boldsymbol{0}$ and voltage magnitudes of all buses are assumed constant at 1.0 per unit. The angle difference between two buses is assumed small such that the $\cos(\theta_{ij}) = 1$ and $\sin(\theta_{ij}) = \theta_i - \theta_j$ [46]. Thus, $\boldsymbol{Q} = \boldsymbol{0}$, and Equation (19) and (21) can be removed from constraints Equation (18) simplifies as follows:

$$P_{ij} = B_{ij}(\theta_i - \theta_j) \ (\forall (i,j) \in \mathcal{B}) \tag{26}$$

2) Quadratic-Convex AC Power Flow Model: Sundar *et al.* introduce several quadratic-convex (QC) relaxation schemes on AC power flow models based on the McCormick envelopes [47] for the square and products of variables [48]. The strengthened quadratic-convex relaxation (QCLS) are applied in this work to obtain the tightest voltage and phase angle difference bounds to efficiently solve the AC problems [48]. A simplified QCLS model from the QC relaxed AC OPF problem is also presented, a more detailed deduction and proof of which can be found in [48].

For the QC relaxation, the non-convex equations of power flows can be relaxed with the non-convex sub-expressions using the bounds on voltage magnitude and angle variables. With the McCormick envelopes and Lifted Nonlinear Cuts [49], the sine and cosine function can be further relaxed and

This article has been accepted for publication in a future issue of this journal, but has not been fully edited. Content may change prior to final publication. Citation information: DOI 10.1109/TPWRS.2022.3168226, IEEE Transactions on Power Systems

bounded. The QCLS model is based on the QC relaxation using an extreme point representation. The definition of the extreme point is as follow: given a set $\boldsymbol{X}$, a point $p \in \boldsymbol{X}$ is extreme if there does not exist two other distinct points p_1, $p_2 \in \boldsymbol{X}$ and a non-negative multiplier $\lambda \in [0,1]$, such that $p=\lambda p_1 + (1-\lambda)p_2$. Then, Sundar *et al.* introduced an extreme-point encoding of trilinear terms with a constrains to link the λ variables in multiple trilinear terms.

For example, let $\varphi(x_1,x_2,x_3)=x_1x_2x_3$ denote a trilinear term with variable bounds $\boldsymbol{x_i^l} \leqslant x_i \leqslant \boldsymbol{x_i^u}$ for all i=1,2,3. Then, let $\boldsymbol{\xi}=<\boldsymbol{\xi_1},...,\boldsymbol{\xi_8}>$ denote the vector of eight extreme points of $[\boldsymbol{x_1^l}, \boldsymbol{x_1^u}]\times [\boldsymbol{x_2^l}, \boldsymbol{x_2^u}]\times [\boldsymbol{x_3^l}, \boldsymbol{x_3^u}]$. The extreme points in $\boldsymbol{\xi}$ are given:

$$\begin{aligned} \boldsymbol{\xi_1} &= (\boldsymbol{x_1^l}, \boldsymbol{x_2^l}, \boldsymbol{x_3^l}), \quad \boldsymbol{\xi_2} = (\boldsymbol{x_1^l}, \boldsymbol{x_2^l}, \boldsymbol{x_3^u}), \\ \boldsymbol{\xi_3} &= (\boldsymbol{x_1^l}, \boldsymbol{x_2^u}, \boldsymbol{x_3^l}), \quad \boldsymbol{\xi_4} = (\boldsymbol{x_1^l}, \boldsymbol{x_2^u}, \boldsymbol{x_3^u}), \\ \boldsymbol{\xi_5} &= (\boldsymbol{x_1^u}, \boldsymbol{x_2^l}, \boldsymbol{x_3^u}), \quad \boldsymbol{\xi_6} = (\boldsymbol{x_1^l}, \boldsymbol{x_2^l}, \boldsymbol{x_3^u}), \\ \boldsymbol{\xi_7} &= (\boldsymbol{x_1^u}, \boldsymbol{x_2^u}, \boldsymbol{x_3^l}), \quad \boldsymbol{\xi_8} = (\boldsymbol{x_1^u}, \boldsymbol{x_2^u}, \boldsymbol{x_3^u}). \end{aligned} \tag{27}$$

Then, the tightest convex envelope of the trilinear term $x_1x_2x_3$ is given by the following,

$$< x_1x_2x_3 >^{\lambda} \equiv \begin{cases} \check{x} = \sum_{k=1}^{8} \lambda_i \varphi(\boldsymbol{\xi_k^1}, \boldsymbol{\xi_k^2}, \boldsymbol{\xi_k^3}) \\ x_i = \sum_{k=1}^{8} \lambda_k \boldsymbol{\xi_k^i} \ \forall i = 1,2,3 \\ \sum_{k=1}^{8} \lambda_k = 1, \lambda_k \geqslant 0 \ \forall k = 1,...,8 \end{cases} \tag{28}$$

where the $\boldsymbol{\xi_k^i}$ is the i^{th} coordinate of the $\boldsymbol{\xi_k}$, the $\check{x}$ is the lifted variables representing the trilinear term.

Then, for each branch (i,j) $\in \mathcal{B}$, the sine and cosine functions in power flow equations are formulated as follows:

$$v_i v_j \cos(\theta_{ij}) =< v_i v_j \widetilde{cs_{ij}} >^{\lambda_{ij}^c} \quad (\forall (i,j) \in \mathcal{B}) \tag{29}$$

$$v_i v_j \sin(\theta_{ij}) =< v_i v_j \widetilde{sn_{ij}} >^{\lambda_{ij}^s} \quad (\forall (i,j) \in \mathcal{B}) \tag{30}$$

where $\widetilde{cs_{ij}}$ and $\widetilde{sn_{ij}}$ are the lifted variables for the cosine and sine functions respectively; the λ_{ij}^c and λ_{ij}^s are used for capturing the convex envelopes in the trilinear terms in the QC relaxations.

QCLS also includes a linking constraint to strengthen the relaxation. For each branch in the system, the linking constraint is as follow:

$$\begin{pmatrix} \lambda_{ij,1}^c + \lambda_{ij,2}^c - \lambda_{ij,1}^s - \lambda_{ij,2}^s \\ \lambda_{ij,3}^c + \lambda_{ij,4}^c - \lambda_{ij,3}^s - \lambda_{ij,4}^s \\ \lambda_{ij,5}^c + \lambda_{ij,6}^c - \lambda_{ij,5}^s - \lambda_{ij,6}^s \\ \lambda_{ij,7}^c + \lambda_{ij,8}^c - \lambda_{ij,7}^s - \lambda_{ij,8}^s \end{pmatrix}^T \begin{pmatrix} v_i^l \cdot v_j^l \\ v_i^l \cdot v_j^u \\ v_i^u \cdot v_j^l \\ v_i^u \cdot v_j^u \end{pmatrix} = 0 \tag{31}$$

QCLS ensures a tightest voltage and phase angle difference bounds for AC OPF problems to efficiently compute a local optimal solution. The QCLS model is in the `PowerModels.jl` [42] library, and it is used with the proposed R_{ECO} OPF for the following cases studies.

IV. Overview of Case Studies and Results

The proposed R_{ECO} OPF is applied to six power system cases: the IEEE 24 Bus Reliability Test System (RTS) [50], the reduced Great Britain (GB) network [51], the 37 Bus case from [52], the IEEE 118 Bus System [50], and two synthetic grids, ACTIVSg200 and ACTIVS500, from [53], [54]. The R_{ECO} OPF is modeled and solved with DC, QCLS, and AC power flow models for each case, respectively, to investigate the feasibility and effectiveness. The optimization problem is built in `Julia` [43], and the solver for the R_{ECO} OPF problem uses *Ipopt* [55] and *Juniper* [56]. A flat start is used to initialize the optimization problem [42]. All cases are solved in a laptop with a 2.4 GHz processor and 8 GB memory. It is important to note here that the proposed R_{ECO} OPF involves several layers of logarithm functions (*concave function*) to formulate the objective function, R_{ECO}. Even the relaxation through *Taylor Expansion* ensures the validity of the problem with the solver [55], [56], it is not guaranteed to have a feasible solution or a global optimal for this nonlinear optimization problem.

All cases are solved with DC and QCLS models. Only ACTIVSg200 and ACTIVSg500 can be solved with AC model. The DC model linearizes the power flow constraints of R_{ECO} OPF, making it feasible to solve all cases. The QCLS model tightens the voltage and phase angle difference bounds, which makes the solver efficiently find the local optimal point. Under the original AC power flow boundaries, the flat start cannot guarantee the solution of R_{ECO} OPF since the voltage and phase angle difference have bigger range to search. The feasible boundaries of DC and AC OPF are different [57]. Thus, even though the problem can be solved with DC and QCLS R_{ECO} OPF, it cannot guarantee the feasibility for AC R_{ECO} OPF. The nonlinear objective R_{ECO} would require a better guess of initial point instead of flat start.

TABLE I gives the R_{ECO} OPF results for each case, showing the achieved optimal value of R_{ECO} (Achieved R_{ECO}), the Original R_{ECO}, the computation time, and the solved status. Due to the relaxation of the Taylor Series Expansion, the value of optimal R_{ECO} from the solver is reduced from 0.3678 to 0.3431 for all cases. The **Original R_{ECO}** is based on the original power flows in each case, while the **Achieved R_{ECO}** is based on the R_{ECO} optimized power flows after the control vectors adapting back to the case adapting back to the case and solving it under AC power flow model. This paper adapts a hybrid approach to analyze and compare the effectiveness of different power flow models to R_{ECO} OPF, which is similar to the hybrid approach in [58], [59]. The solution from the solver provides the vectors of V_i, θ_i, P_{gen_i}, and Q_{gen_i} for all buses and generators. We adapt the control vectors back to the system and solve it with AC power flow model through Newton-Raphson method without error. It shows the R_{ECO} OPF under different power flow models are compatible with AC power flow model. Then, we calculate the R_{ECO} through Equation (9)-(13) as the Achieved R_{ECO} indicating the final power systems' state based on the solution. The detailed control vectors and case information have been made publicly available at [60]. With increases in case size and model complexity, solution time increases.

This article has been accepted for publication in a future issue of this journal, but has not been fully edited. Content may change prior to final publication. Citation information: DOI 10.1109/TPWRS.2022.3168226, IEEE Transactions on Power Systems

TABLE I: Results of Ecological Robustness Oriented Power Flow for 6 Power System Networks

Use Case	Power Flow Model	Solved Status	Computation Time (seconds)	Achieved R_{ECO}	Original R_{ECO}
IEEE 24 Bus RTS [50]	DC	Solved	0.35	0.3391	0.3382
IEEE 24 Bus RTS [50]	QCLS	Solved	1.63	0.3395	0.3382
IEEE 24 Bus RTS [50]	AC	Infeasible	NA	NA	0.3382
Reduced GB Network [51]	DC	Solved	28.92	0.3600	0.3441
Reduced GB Network [51]	QCLS	Solved	44.77	0.3581	0.3441
Reduced GB Network [51]	AC	Infeasible	NA	NA	0.3441
37 Bus Case [52]	DC	Solved	0.27	0.2951	0.2846
37 Bus Case [52]	QCLS	Solved	22	0.2972	0.2846
37 Bus Case [52]	AC	Infeasible	NA	NA	0.2846
IEEE 118 Bus System [50]	DC	Solved	61.53	0.3296	0.3064
IEEE 118 Bus System [50]	QCLS	Solved	62.69	0.3201	0.3064
IEEE 118 Bus System [50]	AC	Infeasible	NA	NA	0.3064
ACTIVSg200 [53]	DC	Solved	103.16	0.2496	0.2510
ACTIVSg200 [53]	QCLS	Solved	401.07	0.2506	0.2510
ACTIVSg200 [53]	AC	Solved	1000.19	0.2503	0.2510
ACTIVSg500 [53]	DC	Solved	203.93	0.2236	0.2144
ACTIVSg500 [53]	QCLS	Solved	2140.76	0.2216	0.2144
ACTIVSg500 [53]	AC	Solved	296.83	0.2223	0.2144

Except Reduced GB Network, the Achieved R_{ECO} is lower than 0.3431, the optimal R_{ECO}. That's the error introduced by the change of flow direction and the solvers' settings. For power systems, R_{ECO} depends on both network structure and power flows over the system. A more redundant network structure favors a higher value of R_{ECO}, thus the IEEE 24 Bus RTS and Reduced GB Network have higher original R_{ECO} and the Achieved R_{ECO} than other cases. Analyses of tradeoffs of R_{ECO} with respect to power flow models, system reliability and cost are presented in the following sections.

V. Evaluation and Analyses of R_{ECO} OPF

Several evaluation metrics are introduced here into the case studies to analyze how the R_{ECO} OPF improves the power systems' reliability as well as to study its cost effectiveness.

The results of all analyses are shown in Tables II - IV. Table II and Table III compares reliability, Table IV compares cost-effectiveness, and Table V compares network properties. For simplification, the **Use Case** name in the tables is codefied by its *Case Name*, *Power Flow Model* (DC, QCLS, or AC), and use of R_{ECO} *OPF*. All analyses are done using the AC power flow model with the Newton-Raphson method, with the control vector obtained from `Julia` output. Power system operation feasibility is ensured by solving the AC power flow equations for a feasible operating solution. Once the R_{ECO} OPF problem is solved, no matter using AC, DC or QCLS power flow model, the control vectors are used for generators and bus voltage settings to solve the AC power flow without infeasibility.

A. Contingency Analysis

Contingency analysis is used to examine how the R_{ECO} OPF can improve systems' inherent ability of absorbing disturbances. To compare network reliability, we perform *N-x* contingency analysis for each case with the original operating state and the R_{ECO} optimized operating state. The R_{ECO} OPF is expected to reduce violations under contingencies

The term *N-x contingency analysis* refers to a power system study where, among N total components, x are taken out of service. If the contingency causes operating stress, limit violations occur for different elements, such as branch power flows exceeding thermal limits or bus voltages out of bounds. If the contingency causes the power flow to be unable to be solved, we denote it as unsolved. The contingency analyses are performed considering each case's control settings which are noted, such as droop control, automatic generator control, etc., if present. This modeling is consistent with ARPA-E's requirements for work on grid optimization [61]. Under the same control settings, comparing the quantity of above violations and unsolved situations shows the effectiveness of proposed R_{ECO} OPF to improve power systems' inherent ability of absorbing disturbances and survive from contingencies. It is also important to note that the same case under different operating points can have different levels of survivability against contingencies, and the same contingency can cause different operating violations with different levels of severity. To avoid the endless comparison and discussion of reliability, we use the number of violations and unsolved contingencies

This article has been accepted for publication in a future issue of this journal, but has not been fully edited. Content may change prior to final publication. Citation information: DOI 10.1109/TPWRS.2022.3168226, IEEE Transactions on Power Systems

TABLE II: Reliability Comparison of Ecological Robustness Optimal Power Flow (IEEE 24 Bus RTS, Reduced GB Network, 37 Bus, IEEE 118 System)

Use Case	Achieved R_{ECO}	N-1 Branch	N-1 Generator	N-1 Bus	N-2 Branch
IEEE 24 Bus RTS	0.3382	4 violations	0	11 violations, 1 unsolved	254 violations, 3 unsolved
IEEE 24 Bus RTS DC R_{ECO} OPF	0.3391	4 violations	0	9 violations	232 violations, 1 unsolved
IEEE 24 Bus RTS QCLS R_{ECO} OPF	0.3395	4 violations	0	8 violations, 1 unsolved	215 violations, 2 unsolved
Reduced GB	0.3441	1502 violations	857 violations	228 violations, 14 unsolved	76581 violations, 47 unsolved
Reduced GB DC R_{ECO} OPF	0.3600	0	0	1 violation	6 violations
Reduced GB QCLS R_{ECO} OPF	0.3581	1 violation	0	3 violations	98 violations
37 Bus Case	0.2846	7 violations	0	15 violations	596 violations
37 Bus Case DC R_{ECO} OPF	0.2951	4 violations	0	7 violations	274 violations
37 Bus Case QCLS R_{ECO} OPF	0.2972	7 violations	0	12 violations	495 violations
IEEE 118	0.3064	1 violation	0	10 violations	240 violations, 4 unsolved
IEEE 118 DC R_{ECO} OPF	0.3296	0	0	0	20 violations
IEEE 118 QCLS R_{ECO} OPF	0.3201	0	0	0	34 violations, 3 unsolved

to represent the reliability and survivability of each case under different operating states through the paper.

The comprehensive *N-1* contingencies for each branch, generator, and bus are considered for the IEEE 24 Bus RTS, Reduced GB Network, 37-Bus Case, and the IEEE 118, as well as *N-2* contingencies with the branches. Since these cases are relatively small, the *N-2* contingencies can cause great impact on the system's operation and security. The contingencies capture those systems' ability of absorbing disturbances. For ACTIVSg200 and ACTIVSg500, we consider the *N-1* contingencies for each branch, generator, bus, and substation, respectively. Since these are large cases, it is hard to perform a complete *N-x* contingency when $x \geqslant 2$. In [25], [26], the authors use graph theory and line outage distribution factors (LODFs) to identify critical *N-x* contingencies for ACTIVSg200 and ACTIVSg500 (multiple branches out of service) that cause the system operational stress. The value of x ranges from 3 to 8, and such branches are widespread. The number of compromised branches and the widespread locations make such contingencies statistically *unexpected* and *adversely stress* the system operation. These contingencies are remarked as *critical contingencies*. It is noted that for *N-1* bus or substation contingencies, all connected devices are disconnected from the system, including the generators, load, and branches. In our case studies, substation outage causes up to 5 elements fail (*N-5*). These contingencies can cause generator unavailability, like during the Texas Winter Energy Crisis [3]. A superset comprising all contingency lists as described above of branch, generator, bus, and substations (*N-1*, *N-2*, and *critical contingencies*) is used to examine each case's inherent ability of absorbing large disturbances under the original and R_{ECO} optimized power flows.

Table II shows the reliability comparisons between R_{ECO} OPF and the original case for IEEE 24 Bus RTS, Reduced GB Network, 37 Bus Case, and IEEE 118 Bus systems. Table III shows the reliability comparisons for the ACTIVSg200 system and the ACTIVSg500 system. Table III differs from Table II because for these larger realistic synthetic cases, the contingency list has been expanded to include the selected *critical N-x* contingencies from [25], [26].

The reliability improves for the IEEE 24 Bus RTS with the R_{ECO} OPF using both DC and QCLS power flow models. For *N-1* bus contingencies, the DC R_{ECO} OPF removes the unsolved contingencies and reduces the violations from 11 to 9. For *N-2* branch contingencies, the DC R_{ECO} OPF reduces 2 unsolved contingencies and 22 violations, while the QCLS R_{ECO} OPF reduces 1 unsolved contingency and 39 violations.

R_{ECO} in the Reduced GB network improves using both DC and QCLS power flow models. The original Reduced GB Network is under stress, so the contingency analysis with *N-1* and *N-2* causes numerous violations and multiple unsolved situations. Thus, the reliability improvement from the R_{ECO} OPF for Reduced GB Network is significant. The DC R_{ECO} OPF removes all the *N-1* contingencies with branches and generators. The violations are reduced under *N-1* bus contingencies from 228 to 1. The violations under *N-2* branch contingencies are also greatly reduced, from 76,581 to 6. The QCLS R_{ECO} OPF removes all *N-1* generator contingencies, reduces the *N-1* branch violations from 1,502 to 1, reduces the *N-1* bus violations from 228 to 3, reduces the *N-2* branch violations from 76,581 to 98. All unsolved situations are resolved using both DC and QCLS R_{ECO} OPF.

The R_{ECO} for the 37-Bus case improves with the R_{ECO} OPF using both DC and QCLS power flow models. The QCLS R_{ECO} OPF has higher R_{ECO} and R_{CF} than DC R_{ECO} OPF. However, the reliability improvement of QCLS R_{ECO} OPF is less than DC R_{ECO} OPF. The DC R_{ECO} OPF reduces the violations of *N-1* Branch and Bus Contingencies from 7 to 4 and from 15 to 7, respectively. It also reduces the violations of *N-2* Branch Contingencies from 596 to 274. The QCLS R_{ECO} OPF only reduces the violations of *N-1* Bus Contingencies from 15 to 12, and the violations of *N-2* Branch Contingencies from 596 to 495.

The original IEEE 118 Bus System has no branch limits in the case, so we insert branch limits of 1000 MVA. For contingency analysis, these branch limits do not introduce line overload violations. All violations are voltage violations. The R_{ECO} improves with the R_{ECO} OPF using both DC and QCLS power flow models (Table I). The DC R_{ECO} OPF improves the reliability more, with higher R_{ECO} than QCLS R_{ECO} OPF. Both DC and QCLS R_{ECO} OPF absorb the impact of the *N-1* contingencies. As for *N-2* contingencies, DC R_{ECO} OPF reduces violations from 240 to 20 with no unsolved situations, and QCLS R_{ECO} OPF reduces violations from 240 to 34 with 3 unsolved situations.

The ACTIVSg200 results show that the R_{ECO} is reduced from R_{ECO} OPF with all models (Table I). The change is small, indicating that the system was already operating closer to the optimal R_{ECO} value in the base case. Correspondingly, the reliability is not improved as the other cases. However, the unsolved situations under the *critical contingencies* are reduced.

R_{ECO} for the ACTIVSg500 system improves under all the power flow models. The *N-1* bus and substation contingency

This article has been accepted for publication in a future issue of this journal, but has not been fully edited. Content may change prior to final publication. Citation information: DOI 10.1109/TPWRS.2022.3168226, IEEE Transactions on Power Systems

TABLE III: Reliability Comparison of Ecological Robustness Optimal Power Flow (ACTIVSg200, ACTIVSg500)

Use Case	Achieved R_{ECO}	N-1 Branch	N-1 Bus	N-1 Substation	Critical Contingencies [25], [26]
ACTIVSg200	0.2510	0	26 violations, 1 unsolved	5 violations, 2 unsolved	1030 violations, 17 unsolved
ACTIVSg200 DC R_{ECO} OPF	0.2496	1 violation	27 violations, 1 unsolved	19 violations, 2 unsolved	1741 violations, 13 unsolved
ACTIVSg200 QCLS R_{ECO} OPF	0.2506	0	27 violations, 1 unsolved	19 violations, 2 unsolved	1355 violations, 15 unsolved
ACTIVSg200 AC R_{ECO} OPF	0.2503	0	27 violations, 1 unsolved	19 violations, 2 unsolved	1720 violations, 13 unsolved
ACTIVSg500	0.2144	38 violations	75 violations	66 violations	52 violations, 8 unsolved
ACTIVSg500 DC R_{ECO} OPF	0.2236	39 violations	73 violations	63 violations	32 violations
ACTIVSg500 QCLS R_{ECO} OPF	0.2216	39 violations	71 violations	61 violations	72 violations
ACTIVSg500 AC R_{ECO} OPF	0.2223	39 violations	74 violations	65 violations	41 violations

analysis show improvement of reliability with less violations. However, the *N-1* branch contingencies analysis shows that the optimized system has one more violation than the original state. The DC and AC R_{ECO} OPFs reduce the violations from 52 to 32 and 41, respectively, with no unsolved situations for the critical *N-x* contingencies. The QCLS R_{ECO} OPF has more violations, with no unsolved situations.

Except ACTIVSg200, all other cases' Achieved R_{ECO} has been increased from their Original R_{ECO}. With the improvement of Achieved R_{ECO}, the system's reliability has been improved from its original operating points with less violations and unsolved contingencies. Except 37 Bus case, the higher R_{ECO} is achieved, the operation scheme is more reliable. Thus, this trends show a positive relationship between R_{ECO} and reliability.

B. Resilience/Cost Tradeoff Analysis

The cost-effectiveness of using R_{ECO} to operate power systems is examined by comparing the cost and reliability against the traditional OPF and SCOPF. The reliability is quantified in terms of the total number of violations, unsolved contingencies, and contingencies with violations from different OPFs using each case's contingency list from Section V-A, which includes both *expected N-1* and *unexpected N-x* contingencies. Cost (formulated in Eq. 32) is based on the generators' real power output (P_i) and their cost function (C_i).

$$Cost = \sum_{i=1}^{G} C_i(P_i) \tag{32}$$

`PowerWorld Simulator` [52] is used to perform the OPF and SCOPF analysis for the power system cases. The unit of cost is converted to $/hr based on the marginal cost $/WMhr and generator's output MW. The set of postulated contingencies for SCOPF are the contingencies performed in Section V-A for each case. The SCOPF solution provides a single dispatch against all specified contingencies without remedial actions. The SCOPF in `PowerWorld Simulator` is solved with three major steps: Initialize the SCOPF problem and control structures (generator and bus setpoints); Contingency analysis and storage of control sensitivity with each violation; SCOPF iteration for each contingency and control action until the maximum iterations [62]. The mitigation of some contingencies can often exacerbate others, thus `PowerWorld Simulator` handles these situations using penalty functions for unenforceable contingencies [52]. The penalty used here is $1,000/hr. The SCOPF in `PowerWorld Simulator` uses a DC power flow model. Two types of SCOPF are compared to better investigate and compare the effectiveness from R_{ECO} OPF: a conventional SCOPF with *N-1* branch contingencies and a more powerful SCOPF with the full *N-x* contingencies from Section V-A. They are labeled as SCOPF *N-1* and SCOPF *N-x* in Table IV and Fig. 3, respectively. The SCOPF *N-x* is expected to provide a more resilient operating state against the adversaries since all *unexpected* contingencies are selected. Thus, their comparison between SCOPF and R_{ECO} OPF is performed to compare the preventative approaches that *explicitly* and *implicitly* consider the contingencies under both *expected* and *unexpected* contingencies, respectively.

Similar to the previous analysis, after obtaining the solution from OPF and SCOPF, we perform the contingency analysis using the AC power flow model for each case. This ensures that all contingencies are considered and provides a clear comparison between OPF, SCOPF, and R_{ECO} OPF about their operating points for disturbances as well as their cost. The control settings of each case remains the same for the contingency analysis to examine the inherent ability of absorbing disturbances with different OPFs. Table IV and Fig. 3 shows the cost and reliability comparisons under R_{ECO} OPF, OPF, and SCOPF. We compare the number of violations, unsolved contingencies, contingencies that cause operating violations (denoted as **Violated Contingencies**) under R_{ECO} OPF, OPF and SCOPF.

There are 12 and 86 *unenforceable* contingencies in SCOPF *N-1* and SCOPF *N-x*, respectively for the IEEE 24 Bus RTS. There is 1 *unenforceable* contingency in SCOPF *N-x* for the Reduced GB Network. This means that the solution is unable to resolve those violations and contingencies under the DC model, and thus the operational cost is penalized with $1,000 per unenforceable contingency. All contingencies are enforceable in SCOPF for the other cases, meaning the solution is able to resolve all violations by re-dispatching generators [52].

There are 12 unenforceable contingency constraints in the SCOPF *N-1* for the IEEE 24 Bus RTS (Fig. 3(a)) and each constraint has a cost of $1,000/hr, resulting in the total cost of $109,554.94/hr. Similarly, the total cost for SCOPF *N-x*, $139,612.49/hr, also includes the 24 unenforceable contingency constraints. While cost for R_{ECO} OPF is about 15% higher than OPF, reliability improves under all contingencies. A major potential benefit of the proposed approach can be seen in its comparison to SCOPF, where the cost for R_{ECO} OPF is lower ($74,945/hr for QCLS) than the cost for SCOPF *N-1* ($109,554.94/hr) and SCOPF *N-x* ($139,612.49/hr), while much fewer violations also occur in QCLS R_{ECO} OPF. The R_{ECO} OPF reduces 15.6% violations, 75% unsolved contingencies, and 9.7% contingencies from the original operating point. The OPF reduces 4.8% violations, 25% unsolved contingencies, and 3.2% contingencies. Both SCOPF N-1 and

This article has been accepted for publication in a future issue of this journal, but has not been fully edited. Content may change prior to final publication. Citation information: DOI 10.1109/TPWRS.2022.3168226, IEEE Transactions on Power Systems

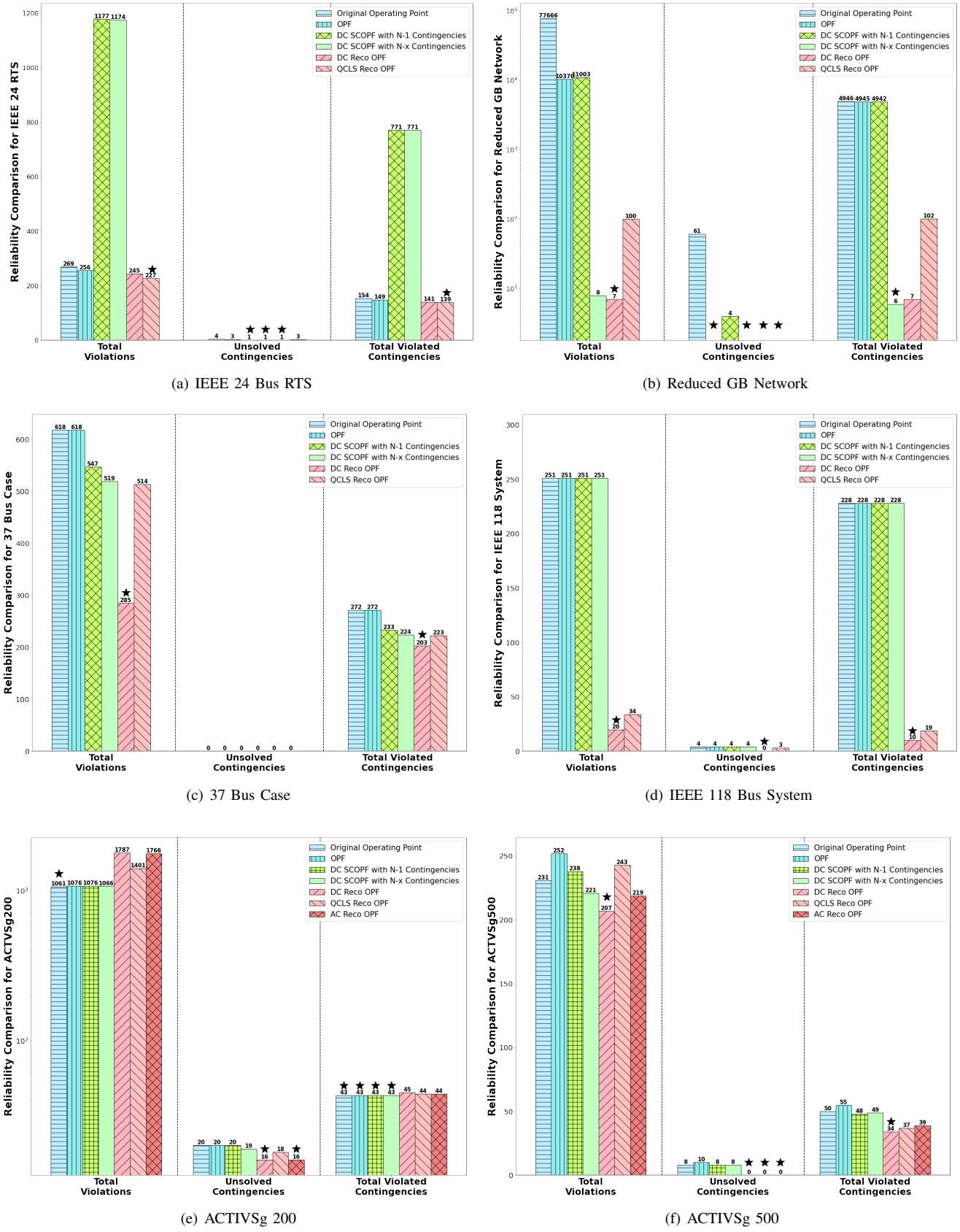

(a) IEEE 24 Bus RTS

(b) Reduced GB Network

(c) 37 Bus Case

(d) IEEE 118 Bus System

(e) ACTIVSg 200

(f) ACTIVSg 500

Fig. 3: Reliability Comparison of Ecological Robustness Optimal Power Flow for all Case Studies. (Note: Y axes have different scaling for better readability)

This article has been accepted for publication in a future issue of this journal, but has not been fully edited. Content may change prior to final publication. Citation information: DOI 10.1109/TPWRS.2022.3168226, IEEE Transactions on Power Systems

TABLE IV: Cost Effectiveness Comparison of Ecological Robustness Optimal Power Flow

Objective	Power Flow Model	Cost($/hr)	Total Violations	Total Unsolved	Violated Contingencies
IEEE 24 Bus RTS					
R_{ECO} OPF	DC	80,582.41	245	1	141
R_{ECO} OPF	QCLS	74,945.96	227	3	139
OPF	AC	63,484.63	256	3	149
SCOPF N-1	DC	109,554.94	1177	1	771
SCOPF *N-x*	DC	139,612.49	1174	1	771
Reduced GB Network					
R_{ECO} OPF	DC	27,805,298	7	0	7
R_{ECO} OPF	QCLS	23,012,295	102	0	100
OPF	AC	7,066,641	10370	0	4945
SCOPF N-1	DC	7,147,613	11462	5	4942
SCOPF *N-x*	DC	7,918,555	8	0	6
37 Bus Case					
R_{ECO} OPF	DC	17,350.07	285	0	202
R_{ECO} OPF	QCLS	18,182.07	514	0	223
OPF	AC	15,809.58	618	0	272
SCOPF N-1	DC	15,846.64	547	0	233
SCOPF *N-x*	DC	15,813.99	519	0	224
IEEE 118 Bus System					
R_{ECO} OPF	DC	48,414.2	20	0	10
R_{ECO} OPF	QCLS	69,895.73	34	3	19
OPF	AC	47,268.54	251	4	228
SCOPF N-1	DC	47,268.54	251	4	228
SCOPF *N-x*	DC	47,268.54	251	4	228
ACTIVSg 200					
R_{ECO} OPF	DC	51,479.93	1787	16	45
R_{ECO} OPF	QCLS	50,265.75	1401	18	44
R_{ECO} OPF	AC	50,850.08	1766	16	44
OPF	AC	48,991.26	1076	20	43
SCOPF N-1	DC	49,144.54	1076	20	43
SCOPF *N-x*	DC	50,237.00	1066	19	43
ACTIVSg 500					
R_{ECO} OPF	DC	89,447.79	207	0	34
R_{ECO} OPF	QCLS	77,159.61	243	0	37
R_{ECO} OPF	AC	77,482.57	219	0	39
OPF	AC	66,287.91	252	10	55
SCOPF N-1	DC	80,025.06	238	8	48
SCOPF *N-x*	DC	94,438.72	221	8	49

N-x reduces 75% unsolved contingencies **but** introduces 400% violations and contingencies. The R_{ECO} OPF is more cost-effective than SCOPF and OPF, while also more effective at absorbing the disturbances, with less violations, unsolved power flow solutions, and contingencies with violations.

Even though the reliability of the Reduced GB Network (Fig. 3(b)) has the most improvement using R_{ECO} OPF, the cost ($27,805,298/hr for QCLS) increases three times as compared to OPF ($6,826,257/hr), SCOPF *N-1* ($7,147,613/hr) and SCOPF *N-x* ($7,918,555/hr). The cost of the single unenforceable contingency constraint is included at $1,000/hr for SCOPF *N-x*. The improvement from OPF and SCOPF *N-1* is very small compared to R_{ECO} OPF and SCOPF *N-1*. Both R_{ECO} OPF and SCOPF *N-x* reduce 99% of violations and contingencies respect to the original operating point and all unsolved contingencies are resolved. For this case, the SCOPF *N-x* appears to be a better option than R_{ECO} OPF. However, the SCOPF depends on postulated contingencies. With more contingencies considered, the SCOPF can prepare a better power dispatch against the contingencies. As comparison, the value of R_{ECO} is its ability to deal with all potential contingencies based on its surprisal model, which includes the unexpected ones.

The cost for R_{ECO} OPF ($17,350.07/hr for DC) for the 37 Bus Case (Fig. 3(c)) is slightly higher than OPF ($15,809.58/hr), SCOPF *N-1* ($15,846.64/hr), and SCOPF *N-x* ($15,813.99/hr). The reliability improvement with R_{ECO} OPF is much greater than OPF and SCOPF. The cost of R_{ECO} OPF is around 10% higher than other OPFs. The R_{ECO} OPF reduced 58% violations and 26% contingencies with respect to its original operating point, SCOPF only reduces 16% violations and 18% contingencies and there is no improvement from OPF. This case exhibits significant cost-effectiveness of the R_{ECO} OPF to improve the reliability of power system operation against unexpected contingencies.

Since the original IEEE 118 Bus System doesn't have branch limits and the inserted 1000 MVA for branch limit is very large, the system won't experience any overflow violations under all contingencies. Thus, the result of SCOPF (DC power flow model) and OPF are the same. For the IEEE 118 Bus System (Fig. 3(d)), the cost for R_{ECO} OPF ($48,414.2/hr for DC) is slightly higher than OPF and SCOPF ($47,268.54/hr). However, the improvement of reliability with R_{ECO} OPF is much greater than OPF and SCOPF. The increased cost is $1,145/hr, which is 10% compared to DC R_{ECO} OPF. However, the reduced violations are 231, which is more than 90% violations reduced. The violated contingencies is also reduced from 228 to 10. With the similar cost, DC R_{ECO} OPF achieves the much better improvement than SCOPF. This case also shows significant cost-effectiveness of using R_{ECO} OPF to improve the reliability of power system operation against unexpected contingencies.

The cost for R_{ECO} OPF ($59,265.75/hr for QCLS) for the ACTIVSg200 case (Fig. 3(e)) is slightly higher than OPF ($48,991.26/hr), SCOPF *N-1* ($49,144.54/hr), and SCOPF *N-x* ($50,237/hr). As discussed in Section V-A, the R_{ECO} of ACTIVSg 200 is not optimized by the proposed R_{ECO} OPF, the reliability is not improved regarding the violations. However, all OPFs do not reduce the violations or violated contingencies respect to the original operating point. Meanwhile, the R_{ECO} OPF reduces the unsolved contingencies with 20% resepct to its original operating point, but SCOPF *N-x* only reduces 5%. The SCOPF *N-1* and OPF have no improvement. Thus, the R_{ECO} OPF can provide more observability to the system when unexpected contingency happen.

The cost for R_{ECO} OPF ($89,447.79/hr for DC) for the ACTIVSg500 case (Fig. 3(f)) is higher than OPF ($66,287.91/hr) and SCOPF *N-1* ($80,025.06/hr) but lower than SCOPF *N-x* ($94,438.72/hr). All R_{ECO} OPF solutions have better reliability regarding total violations and unsolved situations. The R_{ECO}

This article has been accepted for publication in a future issue of this journal, but has not been fully edited. Content may change prior to final publication. Citation information: DOI 10.1109/TPWRS.2022.3168226, IEEE Transactions on Power Systems

OPF reduces 10% violations, 20% unsolved contingencies, and 31% contingencies respect to its original operating point; while the SCOPF reduces 5% unsolved contingencies but introduces 3% violations. The OPF even worsen the reliability. From the cost perspective, the R_{ECO} OPF achieves a lower operating cost than SCOPF *N-x* with a more reliable state. This case also shows the cost-effectiveness of using R_{ECO} OPF for power system operation.

The analysis shows that the improvement of reliability using SCOPF depends on the postulated contingencies. The SCOPF *N-x* is generally more reliable than SCOPF *N-1* because more contingencies are included in the postulated contingency list. The conventional SCOPF *N-1* is not as reliable as the SCOPF *N-x* and proposed R_{ECO} OPF. For all cases, except the Reduced GB Network, the operational cost of R_{ECO} OPF is slightly higher or even less than the DC SCOPF and OPF. The increased cost has also been justified with many fewer violations and unsolved contingencies, contributing to much better reliability. The IEEE 24 RTS, 37 Bus case, IEEE 118 Bus System, and ACTIVSg500 cases show the improvement of reliability from R_{ECO} OPF are much better than SCOPF *N-x*.

C. Power Network Robustness (R_{CF}) and Power Flow Distribution Properties

Koç *et al.* introduced an entropy-based network robustness metric (R_{CF}) in [18]. The R_{CF} is used to identify the potential of cascading failures in power systems, which depends on the network topology and power flow dispatch over the system. A more homogeneous power flow distribution across lines has been shown to increase robustness with respect to cascading link overload failures, while a relatively heterogeneous power flow distribution increases the chance of link overload failure spread [14], [15], [18]. Hence, a system with higher R_{CF} may be less likely to experience cascading failures. The comparison with R_{CF} can also capture how likely the system will experience cascading failures with R_{ECO} optimized power flow.

The calculation of R_{CF} is as follows,

$$R_{CF} = \sum_{i=1}^{N} R_{n,i}\delta_i \tag{33}$$

$$R_{n,i} = -\sum_{i=1}^{L} \alpha_i p_i log(p_i) \quad and \quad \delta_i = \frac{P_i}{\sum_{j=1}^{N} P_j} \tag{34}$$

where α_i is the ratio between the maximum capacity and the load of corresponding line i; p_i is the normalized flow values on the out-going links; P_i is the total power distributed by node i and N is the number of nodes in the network.

The optimal R_{ECO} OPF should guide a more balanced pathway efficiency and redundancy for power flows. Thus, we would expect the power flows to be more equally distributed over the system. Hence, we also compute and compare the distribution of power flows over the system by analyzing the *Mean* and *Standard Deviation (STD)* of the apparent power (MVA) and the line percentage (MVA%) in all branches. The MVA is the apparent power, and the MVA% is the MVA divided by the branch limit. Equation (35) show the calculation of *Mean* and *STD*, respectively, where x_i is each branch's MVA, and x_i is the i^{th} branch's MVA%. The *N* is the total number of branches.

$$\overline{x} = \frac{1}{N}\sum_{i=i}^{n} x_i \; ; \quad s(x) = \sqrt{\frac{1}{N-1}\sum_{i=1}^{N}(x_i - \overline{x})^2} \tag{35}$$

TABLE V: Network Property Comparison of Ecological Robustness Optimal Power Flow

Use Case	R_{CF}	Mean(MVA)	STD(MVA)	Mean(MVA%)	STD(MVA%)
IEEE 24 Bus RTS	1.121	124.07	84.84	32.36	19.04
IEEE 24 Bus RTS DC R_{ECO} OPF	1.330	106.80	68.13	28.54	17.27
IEEE 24 Bus RTS QCLS R_{ECO} OPF	1.289	110.36	67.97	29.27	17.03
Reduced GB	1.058	1356.94	1127.53	60.68	36.52
Reduced GB DC R_{ECO} OPF	4.311	394.74	361.08	16.48	11.56
Reduced GB QCLS R_{ECO} OPF	3.423	450.14	401.44	18.64	13.23
37 Bus Case	1.246	45.73	34.06	34.06	16.3
37 Bus Case DC R_{ECO} OPF	1.386	36.36	26.79	30.26	15.94
37 Bus Case QCLS R_{ECO} OPF	1.452	38.3	25.07	29.67	20.7
IEEE 118	6.866	55.76	66.92	5.7	6.72
IEEE 118 DC R_{ECO} OPF	8.532	38.51	39.71	4	4
IEEE 118 QCLS R_{ECO} OPF	5.602	55.07	75.42	5.61	7.57
ACTIVSg200	1.565	39.08	57	18.01	19.06
ACTIVSg200 DC R_{ECO} OPF	1.535	38.77	56.21	17.55	17.78
ACTIVSg200 QCLS R_{ECO} OPF	1.552	38.53	58.42	17.18	17.29
ACTIVSg200 AC R_{ECO} OPF	1.541	38.44	56.89	17.44	17.42
ACTIVSg500	2.116	54.17	77.1	22.53	17.74
ACTIVSg500 DC R_{ECO} OPF	2.433	48.29	57.91	21.47	17.05
ACTIVSg500 QCLS R_{ECO} OPF	2.455	48.87	59.94	21.63	17.07
ACTIVSg500 AC R_{ECO} OPF	2.393	49.41	67.41	21.52	17.2

Table V shows the network property comparisons between R_{ECO} OPF and the original operation status for all cases.

For the IEEE 24 Bus RTS, the R_{ECO} OPF improves the robustness R_{CF} with respect to the original state. This result is reinforced by results from the analysis of flow distribution properties using MVA and MVA%. The R_{ECO} optimized power flow has a decreased *Mean* and *STD* of MVA and MVA% from the original state. The flow is more equally distributed in a more homogeneous power flow distribution after the optimization. It is observed that the DC R_{ECO} OPF has a higher R_{CF} of 1.330, compared to 1.289 for QCLS (Table V), but a slightly lower R_{ECO} of 0.3391 compared to 0.3395 (QCLS) (Table I). The difference comes from the perspectives of these two metrics. The R_{ECO} analyzes power system robustness from an ecological perspective to examine the pathway efficiency and redundancy, while the R_{CF} focuses on the power flow ingress and egress from each node. Similarly, it is observed the

This article has been accepted for publication in a future issue of this journal, but has not been fully edited. Content may change prior to final publication. Citation information: DOI 10.1109/TPWRS.2022.3168226, IEEE Transactions on Power Systems

Mean(MVA) and *Mean(MVA%)* of DC R_{ECO} OPF is smaller (more homogeneous) than the QCLS R_{ECO} OPF, while the *STD(MVA)* and *STD(MVA%)* of DC R_{ECO} OPF is larger (less homogeneous) than the QCLS R_{ECO} OPF.

For the Reduced GB Network, the R_{ECO} OPF improves the R_{CF} from the original state. The R_{ECO} optimized power flow distribution has smaller *Mean* and *STD* of MVA and MVA% than the original state. The DC R_{ECO} OPF has a higher R_{CF} of 4.311, compared to 3.423 for QCLS (Table V), and its R_{ECO} is 0.36, which is also higher than 0.3518 for QCLS (Table I). The *Mean* and *STD* of MVA and MVA% of DC R_{ECO} OPF are smaller than QCLS R_{ECO} OPF. Thus, the DC R_{ECO} OPF provides a more robust state whose power flows are more equally distributed.

For the 37 Bus Case, QCLS R_{ECO} OPF has higher value of R_{CF} (1.452) and R_{ECO} (0.2972) than their values in DC R_{ECO} (1.386 and 0.2951, respectively). However, DC R_{ECO} OPF has smaller *Mean(MVA)* and *STD(MVA%)* than QCLS R_{ECO} OPF. In particular, the *STD(MVA%)* of DC R_{ECO} OPF is much smaller than QCLS R_{ECO} OPF, which contributes to its reliability improvement as the power flow is more homogeneous.

For the IEEE 118 Bus System, the DC R_{ECO} OPF has smaller *Mean* and *STD* of both MVA and MVA% than the original operating point, with a higher value of R_{CF} (8.532) and R_{ECO} (0.3296). However, the *STD(MVA)* and *STD(MVA%)* of QCLS R_{ECO} OPF are higher than the original case and have a lower value of R_{CF} (5.602) but a higher value of R_{ECO} (0.3201). Since the MVA limits are the same for all branches, the calculation of R_{CF} only depends on the power flow. For QCLS R_{ECO} OPF, the decrease of R_{CF} (from 6.866 to 5.602) shows that the power flow is less equally distributed than the original case, but the R_{ECO} increases (from 0.3064 to 0.3201), which shows the power flow is more balanced between pathway efficiency and redundancy. The improvement of reliability for the IEEE 118 Bus System suggests that a power system with a more balanced pathway efficiency and redundancy can improve the system's inherent ability of absorbing disturbances even the power flow is distributed less homogeneous.

The R_{CF} for the optimized ACTIVSg200 systems are also reduced by a small amount, suggesting that the system is more inclined to have cascading failures. However, the smaller *Mean(MVA%)* and *STD(MVA%)* suggest the power flow is more equally distributed. All the comparisons suggest that power systems with a more balanced pathway efficiency and redundancy operating state have better reliability and resilience under contingencies. As mentioned earlier, the proposed R_{ECO} OPF includes the relaxation of R_{ECO}. From the analysis with ACTIVSg200 system, whose reliability and R_{ECO} worsen after the optimization, it appears that this case was already closer to its true theoretical optimal R_{ECO} than our solution using the relaxation was able to achieve.

For the ACTIVSg500 system, the R_{ECO} optimized systems have more equally distributed power flow as well as increased R_{CF}. Thus, the system is less likely to have cascading failures. The improvements under different models are close, but there are some discrepancies among the analyses with R_{CF}, R_{ECO} and the *Mean* and *STD* of MVA and MVA% about their improvement in the system. This shows that the R_{ECO} can provide a new perspective to assess the system's resilience to unexpected extreme events.

From all cases, there is a positive correlation between R_{ECO} and R_{CF} where a higher R_{ECO} corresponds to a higher R_{CF}. It indicates that the R_{ECO} optimized system provides a more homogeneous power flows that contributes to its improvement of survivability and resilience.

VI. Discussion

The effectiveness and cost-effectiveness of the proposed R_{ECO} OPF is demonstrated with these case studies and analyses. The optimized system has better reliability against different levels of contingencies, the power flow is more equally distributed, and they are less likely to experience cascading failures. Compared with traditional OPF and SCOPF, the operation cost induced by R_{ECO} OPF has been validated by its improvement of reliability with less violations and unsolved situations under unexpected contingencies.

The R_{ECO} OPF for the four small cases presented cannot be solved under an AC power flow model. However, the other two larger cases can be solved using the AC model. Thus, the way how to guarantee the feasibility of the problem and solve the problem with AC power flow model need to be analyzed. One way to obtain the AC power flow solution is to relax the formulation of AC power flow. This paper utilizes a quadratic-convex relaxation on the power flow model (QCLS) for obtaining tighter bounds for voltage and phase angle difference, and it has been successfully solved with all cases. Other approaches of obtaining a valid solution for AC power flow model can also be explored in future work, such as formulating the problem for a better nonlinear program solver, determining a better start point for the local optimal, and using a data-driven approach to solve the problem more efficiently.

The ACTIVSg200 and the IEEE 24 Bus RTS QCLS solutions are better than their DC solutions, with overall fewer violations and violated contingencies (Table IV), as seen from the reliability comparison among the different power flow models' R_{ECO} OPF. The rest of the cases' DC R_{ECO} OPF solutions improve the system's reliability more than their AC or QCLS solutions. The improvement of survivability against contingencies depends on both the R_{ECO} OPF and the system's devices control mechanisms. Considering each system's control mechanisms, whether the AC or DC power flow model is used, and the system's reactive power characteristics will also influence the system's improvement with R_{ECO} OPF.

The economic-driven OPF and SCOPF are used for the cost-effectiveness analysis as benchmarks to investigate how much the reliability improvement can be and how much it will cost for R_{ECO} OPF at the operation planning stage. Advantages of R_{ECO} OPF against SCOPF have been observed, with larger reliability improvements for the IEEE 24 RTS, 37 Bus, IEEE 118 Bus System, and ACTIVSg 500 cases. The effectiveness between R_{ECO} OPF and SCOPF *N-x* for the Reduced GB network is very close, but R_{ECO} OPF is still much better than the conventional SCOPF *N-1*. Even

This article has been accepted for publication in a future issue of this journal, but has not been fully edited. Content may change prior to final publication. Citation information: DOI 10.1109/TPWRS.2022.3168226, IEEE Transactions on Power Systems

though the number of violations and contingencies are almost the same of R_{ECO} OPF and SCOPF *N-x* in the Reduced GB network studies, the severity of contingencies are different. As we mentioned in Section V-A, the same contingency can cause different operating violations with different levels of severity. However, with six cases in the paper it is preferred to use *one* specific standard, the number of violations and contingencies, to demonstrate the effectiveness for R_{ECO} OPF. A more in-depth analysis regarding severity of contingency can be discussed in future work.

Two types of SCOPF are compared with R_{ECO} OPF with regards to cost and reliability. The SCOPF *N-1*, representing the conventional SCOPF, considers *N-1* contingencies in the postulated contingency list, and the SCOPF *N-x* considers all *N-x* contingencies (Section VA), which should greatly increase SCOPF's ability to deal with all contingencies. The results show that the SCOPF *N-x* is generally more reliable than the SCOPF *N-1*. This also proves that SCOPF depends on the postulated contingencies, so it targets specific contingencies; by contrast, the R_{ECO} OPF optimizes the power flow dispatch against unseen potential contingencies. Thus, the comparison between SCOPF *N-x* and R_{ECO} OPF in this paper is the comparison of *explicitly* and *inexplicably* considering potential contingencies. Even with these additions to SCOPF, we still observe that most R_{ECO} optimized cases are more reliable with less violated contingencies, violations, and unsolved contingencies. This exhibits the great *potential* for replacing SCOPF with R_{ECO} OPF to help achieve long-term power system resilience.

The purpose of R_{ECO} OPF is to help improve power system planning against unknown hazards by designing in operational resilience. The economics-driven OPF and SCOPF are useful benchmarks for our method with what is done now regarding reliability and economics in power system planning. The choice of whether and how to implement the R_{ECO} OPF, either as an alternative to SCOPF or with SCOPF, depends on how stakeholders understand the underlying benefits of R_{ECO} OPF against all potential contingencies and how much they are willing to pay in operational cost. SCOPF and R_{ECO} OPF can be used in a way that is complementary. Modern power systems consist of cyber and physical networks that are exposed to different levels of threats and contingencies, including from extreme weather, aging infrastructure, and coordinated attacks. The decision to use R_{ECO} OPF and/or another planning approach depends on the stakeholders and outside information, such as: how much the stakeholders are willing to pay for *expected* contingencies, how much they are willing to pay for *unexpected* contingencies, and how accurately they can predict the expected contingencies decide when to use the R_{ECO} OPF or SCOPF. Both methodologies help toward improving power system resilience against hazards, and future work can design how this would look.

Even though five cases show the effectiveness of using R_{ECO} to improve the system's reliability, there is one case (ACTIVSg200) that results in a reduced R_{ECO} after the optimization. R_{ECO} depends on both network structure and power flows in the system. Due to the relaxation of R_{ECO} as we build the optimization model, the effectiveness may be reduced in certain for ACTIVSg200 where the R_{ECO} is already close to its optimal value. This emphasizes the need of constructing a more strict objective function for R_{ECO}. However, the analysis of ACTIVSg200 case also shows the relationship between R_{ECO} and power system reliability: for each case's operating status, the improved *Achieved* R_{ECO} improves the reliability; while the worsened *Achieved* R_{ECO} impairs the reliability. Additionally, the proposed R_{ECO} OPF algorithm does not include economic factors in the formulation. Even though the cost-effectiveness is observed from four cases in the paper, the R_{ECO} OPF can be further developed with direct consideration of operational cost to ensure and improve its R_{ECO} as well as cost-effectiveness.

VII. Conclusion

Inspired from ecosystems, whose long-term survivability against disturbances benefits from its unique network structure and energy flow pathways, this paper presents a R_{ECO}-oriented OPF problem. It provides a new objective for resilient power system operation. The proposed R_{ECO} OPF guides the power flow dispatch to achieve a balance of power flow pathway *efficiency* and *redundancy* for a more resilient state. In this way, the system enhances its inherent ability of absorbing disturbances without remedial actions. Due to the complexity of R_{ECO}'s formulation, we apply a Taylor Series Expansion for the logarithm function. In this way, we have successfully solved the proposed R_{ECO} OPF with six standard power system cases under different power flow models. With case studies, we observe the effectiveness of using R_{ECO} to represent and improve power systems' inherent resilience against unexpected disturbances. With comparisons to OPF and SCOPF, this paper also shows the cost-effectiveness of using R_{ECO} to guide the power flow dispatch. With the analysis of R_{CF} and the *Mean* and *STD* of power flows, the R_{ECO} OPF makes the power flow more equally distributed over the system. This also improves the system's resilience against cascading failures.

As the first effort to use the inspiration of ecosystems to guide power systems operation for improved resilience, the future work can be developed in following directions: (1) To validate the feasibility and efficiency of the proposed R_{ECO} OPF for various cases with different solvers and start points; (2) To formulate a more strict R_{ECO} for the objective function and ensure its feasibility for large systems; (3) To formulate operational algorithms that consider both state-of-the-art SCOPF and R_{ECO} OPF against expected and unexpected contingencies for power system resilience; (4) To propose an enhanced R_{ECO} OPF with economic factors that ensure its cost-effectiveness while finding a balance of operational cost and long-term suvivability against unexpected contingencies; and (5) To consider high penetration of renewables and the stochastic nature of renewable energy with the R_{ECO} OPF model, to better power systems' operation for economy, environment, and survivability.

Acknowledgment

The authors would like to acknowledge the US Department of Energy Cybersecurity for Energy Delivery Systems program

under award DE-OE0000895 and the National Science Foundation under Grant 1916142 for their support of this work.

REFERENCES

[1] M. B. Cain, R. P. O'neill, A. Castillo *et al.*, "History of optimal power flow and formulations," *Federal Energy Regulatory Commission*, vol. 1, pp. 1–36, 2012.

[2] F. Capitanescu, J. M. Ramos, P. Panciatici, D. Kirschen, A. M. Marcolini, L. Platbrood, and L. Wehenkel, "State-of-the-art, challenges, and future trends in security constrained optimal power flow," *Electric Power Systems Research*, vol. 81, no. 8, pp. 1731–1741, 2011.

[3] I. Ivanova, "Texas winter storm costs could top $200 billion - more than hurricanes Harvey and Ike," Feb 2021. [Online]. Available: https://www.cbsnews.com/news/texas-winter-storm-uri-costs

[4] National Academies of Sciences, Engineering, and Medicine, *Enhancing the Resilience of the Nation's Electricity System*. Washington, DC: The National Academies Press, 2017. [Online]. Available: https://www.nap.edu/catalog/24836/enhancing-the-resilience-of-the-nations-electricity-system

[5] L. Das, S. Munikoti, B. Natarajan, and B. Srinivasan, "Measuring smart grid resilience: Methods, challenges and opportunities," *Renewable and Sustainable Energy Reviews*, vol. 130, p. 109918, 2020.

[6] M. Panteli, P. Mancarella, D. N. Trakas, E. Kyriakides, and N. D. Hatziargyriou, "Metrics and quantification of operational and infrastructure resilience in power systems," *IEEE Transactions on Power Systems*, vol. 32, no. 6, pp. 4732–4742, 2017.

[7] M. Panteli and P. Mancarella, "Modeling and evaluating the resilience of critical electrical power infrastructure to extreme weather events," *IEEE Systems Journal*, vol. 11, no. 3, pp. 1733–1742, 2015.

[8] B. Cai, M. Xie, Y. Liu, Y. Liu, and Q. Feng, "Availability-based engineering resilience metric and its corresponding evaluation methodology," *Reliability Engineering & System Safety*, vol. 172, pp. 216–224, 2018.

[9] A. Monticelli, M. Pereira, and S. Granville, "Security-constrained optimal power flow with post-contingency corrective rescheduling," *IEEE Transactions on Power Systems*, vol. 2, no. 1, pp. 175–180, 1987.

[10] A. Marano-Marcolini, F. Capitanescu, J. L. Martinez-Ramos, and L. Wehenkel, "Exploiting the use of dc scopf approximation to improve iterative ac scopf algorithms," *IEEE Transactions on Power Systems*, vol. 27, no. 3, pp. 1459–1466, 2012.

[11] F. Capitanescu, "Approaches to obtain usable solutions for infeasible security-constrained optimal power flow problems due to conflicting contingencies," in *2019 IEEE Milan PowerTech*. IEEE, 2019, pp. 1–6.

[12] E. Karangelos and L. Wehenkel, "An iterative ac-scopf approach managing the contingency and corrective control failure uncertainties with a probabilistic guarantee," *IEEE Transactions on Power Systems*, vol. 34, no. 5, pp. 3780–3790, 2019.

[13] I.-I. Avramidis, F. Capitanescu, S. Karagiannopoulos, and E. Vrettos, "A novel approximation of security-constrained optimal power flow with incorporation of generator frequency and voltage control response," *IEEE Transactions on Power Systems*, vol. 36, no. 3, pp. 2438–2447, 2020.

[14] Y. Wang, L. Huang, M. Shahidehpour, L. L. Lai, H. Yuan, and F. Y. Xu, "Resilience-constrained hourly unit commitment in electricity grids," *IEEE Transactions on Power Systems*, vol. 33, no. 5, pp. 5604–5614, 2018.

[15] Y. Wang, L. Huang, M. Shahidehpour, L. L. Lai, and Y. Zhou, "Impact of cascading and common-cause outages on resilience-constrained optimal economic operation of power systems," *IEEE Transactions on Smart Grid*, vol. 11, no. 1, pp. 590–601, 2019.

[16] D. N. Trakas and N. D. Hatziargyriou, "Resilience constrained day-ahead unit commitment under extreme weather events," *IEEE Transactions on Power Systems*, vol. 35, no. 2, pp. 1242–1253, 2019.

[17] T. Zhao, H. Zhang, X. Liu, S. Yao, and P. Wang, "Resilient unit commitment for day-ahead market considering probabilistic impacts of hurricanes," *IEEE Transactions on Power Systems*, vol. 36, no. 2, pp. 1082–1094, 2020.

[18] Y. Koç, M. Warnier, R. E. Kooij, and F. M. Brazier, "An entropy-based metric to quantify the robustness of power grids against cascading failures," *Safety science*, vol. 59, pp. 126–134, 2013.

[19] Y. Xiang, L. Wang, and N. Liu, "A robustness-oriented power grid operation strategy considering attacks," *IEEE transactions on smart grid*, vol. 9, no. 5, pp. 4248–4261, 2017.

[20] K. Lai, Y. Wang, D. Shi, M. S. Illindala, Y. Jin, and Z. Wang, "Sizing battery storage for islanded microgrid systems to enhance robustness against attacks on energy sources," *Journal of Modern Power Systems and Clean Energy*, vol. 7, no. 5, pp. 1177–1188, 2019.

[21] R. Lai, X. Qiu, and J. Wu, "Robustness of asymmetric cyber-physical power systems against cyber attacks," *IEEE Access*, vol. 7, pp. 61 342–61 352, 2019.

[22] Y. Zhang, M. E. Raoufat, and K. Tomsovic, "Remedial action schemes and defense systems," *Smart grid handbook*, pp. 1–10, 2016.

[23] S. Hossain-McKenzie, M. Kazerooni, K. Davis, S. Etigowni, and S. Zonouz, "Analytic corrective control selection for online remedial action scheme design in a cyber adversarial environment," *IET Cyber-Physical Systems: Theory & Applications*, vol. 2, no. 4, pp. 188–197, 2017.

[24] H. Huang, M. Kazerooni, S. Hossain-McKenzie, S. Etigowni, S. Zonouz, and K. Davis, "Fast generation redispatch techniques for automated remedial action schemes," in *2019 20th International Conference on Intelligent System Application to Power Systems (ISAP)*. IEEE, 2019, pp. 1–8.

[25] M. R. Narimani, H. Huang, A. Umunnakwe, Z. Mao, A. Sahu, S. Zonouz, and K. Davis, "Generalized contingency analysis based on graph theory and line outage distribution factor," *IEEE Systems Journal*, 2021.

[26] H. Huang, Z. Mao, M. R. Narimani, and K. R. Davis, "Toward efficient wide-area identification of multiple element contingencies in power systems," in *2021 IEEE Power & Energy Society Innovative Smart Grid Technologies Conference (ISGT)*. IEEE, 2021, pp. 01–05.

[27] A. Sahu, P. Wlazlo, Z. Mao, H. Huang, A. Goulart, K. Davis, and S. Zonouz, "Design and evaluation of a cyber-physical testbed for improving attack resilience of power systems," *IET Cyber-Physical Systems: Theory & Applications*, 2021.

[28] R. E. Ulanowicz, "Quantitative methods for ecological network analysis," *Computational Biology and Chemistry*, vol. 28, no. 5, pp. 321–339, 2004.

[29] B. D. Fath, U. M. Scharler, R. E. Ulanowicz, and B. Hannon, "Ecological network analysis: network construction," *Ecological modelling*, vol. 208, no. 1, pp. 49–55, 2007.

[30] R. E. Ulanowicz, S. J. Goerner, B. Lietaer, and R. Gomez, "Quantifying sustainability: resilience, efficiency and the return of information theory," *Ecological complexity*, vol. 6, no. 1, pp. 27–36, 2009.

[31] V. Panyam, H. Huang, B. Pinte, K. Davis, and A. Layton, "Bio-inspired design for robust power networks," in *2019 IEEE Texas Power and Energy Conference (TPEC)*. IEEE, 2019, pp. 1–6.

[32] V. Panyam, H. Huang, K. Davis, and A. Layton, "Bio-inspired design for robust power grid networks," *Applied Energy*, vol. 251, p. 113349, 2019.

[33] H. Huang, V. Panyam, M. R. Narimani, A. Layton, and K. R. Davis, "Mixed-integer optimization for bio-inspired robust power network design," in *2020 52nd North American Power Symposium (NAPS)*. IEEE, 2021, pp. 1–6.

[34] H. Huang, V. Panyam, M. Zeyu, A. Layton, and K. R. Davis, "An ecological robustness-oriented approach for power system network expansion," *arXiv preprint arXiv:updated*, 2021.

[35] A. Layton, "Food webs: realizing biological inspirations for sustainable industrial resource networks," Ph.D. dissertation, Georgia Institute of Technology, 2014.

[36] R. E. Ulanowicz, S. J. Goerner, B. Lietaer, and R. Gomez, "Quantifying sustainability: Resilience, efficiency and the return of information theory," *Ecol. Complex.*, vol. 6, no. 1, pp. 27–36, 2009.

[37] A. Bodini and B. Cristina, "Bodini 2002 sustainanble-water resource-wholesystem.pdf," *Int. J. Environ. Pollut.*, vol. 18, no. 5, pp. 463–485, 2002.

[38] R. E. Ulanowicz, "An Hypothesis on the Development of Natural Communities," *J. theor. Biol*, vol. 85, pp. 223–245, 1980.

[39] R. W. Rutledge, B. L. Basore, and R. J. Mulholland, "Ecological stability: an information theory viewpoint," *Journal of Theoretical Biology*, vol. 57, no. 2, pp. 355–371, 1976.

[40] J. Cohen, R. Beaver, S. Cousins, D. DeAngelis, L. Goldwasser, K. Heong, R. Holt, A. Kohn, J. Lawton, N. Martinez *et al.*, "Improving food webs," *Ecology*, vol. 74, no. 1, pp. 252–258, 1993.

[41] R. E. Ulanowicz and J. S. Norden, "Symmetrical overhead in flow networks," *International Journal of Systems Science*, vol. 21, no. 2, pp. 429–437, 1990.

[42] C. Coffrin, R. Bent, K. Sundar, Y. Ng, and M. Lubin, "Powermodels. j1: An open-source framework for exploring power flow formulations," in *2018 Power Systems Computation Conference (PSCC)*. IEEE, 2018, pp. 1–8.

[43] Juliaopt. [Online]. Available: https://www.juliaopt.org/

[44] K. G. Binmore and K. G. Binmore, *Mathematical Analysis: a straightforward approach*. Cambridge University Press, 1982.

This article has been accepted for publication in a future issue of this journal, but has not been fully edited. Content may change prior to final publication. Citation information: DOI 10.1109/TPWRS.2022.3168226, IEEE Transactions on Power Systems

[45] Z. Jin and G. Jin, *Mathematical analysis*. Dalian University of Technology Press Dalian, 2007.
[46] J. Duncan Glover, M. Sarma, and T. Overbye, *Power System Analysis and Design*, 5th ed. Cengage Learning, 2012.
[47] G. P. McCormick, "Computability of global solutions to factorable nonconvex programs: Part i—convex underestimating problems," *Mathematical programming*, vol. 10, no. 1, pp. 147–175, 1976.
[48] K. Sundar, H. Nagarajan, S. Misra, M. Lu, C. Coffrin, and R. Bent, "Optimization-based bound tightening using a strengthened qc-relaxation of the optimal power flow problem," *arXiv preprint arXiv:1809.04565*, 2018.
[49] C. Coffrin, H. L. Hijazi, and P. Van Hentenryck, "Strengthening the sdp relaxation of ac power flows with convex envelopes, bound tightening, and valid inequalities," *IEEE Transactions on Power Systems*, vol. 32, no. 5, pp. 3549–3558, 2016.
[50] R. D. Zimmerman, C. E. Murillo-Sánchez, and R. J. Thomas, "Matpower: Steady-state operations, planning, and analysis tools for power systems research and education," *IEEE Transactions on power systems*, vol. 26, no. 1, pp. 12–19, 2010.
[51] W. Bukhsh and K. McKinnon, "Network data of real transmission networks," *Published online at http://www. maths. ed. ac. uk/optenergy/NetworkData*, 2013.
[52] PowerWorld Corporation, available at http://www.powerworld.com, 2018.
[53] "Electric grid test case repository." [Online]. Available: https://electricgrids.engr.tamu.edu/
[54] A. B. Birchfield, T. Xu, K. M. Gegner, K. S. Shetye, and T. J. Overbye, "Grid structural characteristics as validation criteria for synthetic networks," *IEEE Transactions on Power Systems*, vol. 32, no. 4, pp. 3258–3265, 2017.
[55] A. Wächter and L. T. Biegler, "On the implementation of an interior-point filter line-search algorithm for large-scale nonlinear programming," *Mathematical programming*, vol. 106, no. 1, pp. 25–57, 2006.
[56] O. Kröger, C. Coffrin, H. Hijazi, and H. Nagarajan, "Juniper: An open-source nonlinear branch-and-bound solver in julia," in *International Conference on the Integration of Constraint Programming, Artificial Intelligence, and Operations Research*. Springer, 2018, pp. 377–386.
[57] K. Baker, "Solutions of dc opf are never ac feasible," in *Proceedings of the Twelfth ACM International Conference on Future Energy Systems*, 2021, pp. 264–268.
[58] S. Kim and T. J. Overbye, "Hybrid power flow analysis: Combination of ac and dc models," in *2011 IEEE Power and Energy Conference at Illinois*. IEEE, 2011, pp. 1–4.
[59] ——, "Mixed power flow analysis using ac and dc models," *IET generation, transmission & distribution*, vol. 6, no. 10, pp. 1053–1059, 2012.
[60] "Bio-Inspired Design of Complex Energy Systems," 2021. [Online]. Available: https://katedavis.engr.tamu.edu/projects/bio-inspired-design-of-complex-energy-systems/
[61] ARPA-E, "SCOPF Problem Formulation: Challenge 1, Grid Optimization Competition," 2019. [Online]. Available: https://gocompetition.energy.gov/challenges/challenge-1/formulation
[62] "SCOPF Solution Process," 2021. [Online]. Available: https://www.powerworld.com/WebHelp/Content/MainDocumentation_HTML/SCOPF_Solution_Process.htm

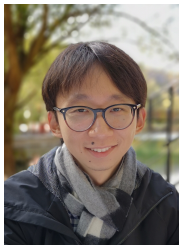

Hao Huang (Student Member, IEEE) : received the B.S. degree in Electrical Engineering (Power System and Its Automation) from Harbin Institute of Technology, Harbin, Heilongjiang Province, China, in 2014 and the M.S. degree in Electrical Engineering (Electric Power) from University of Southern California, Los Angeles, CA, USA, in 2016. He is currently pursuing a Ph.D. degree in Electrical Engineering at Texas A&M University with Prof. Katherine Davis. His research focuses on power system resilience, power system situational awareness, cyber-physical security, etc.

Zeyu Mao (Graduate Student Member, IEEE) received the B.S. degree in electrical engineering from Chongqing University, Chongqing, China, in 2015, and the M.S. degree in electrical and computer engineering from the University of Illinois at Urbana–Champaign, IL, USA, in 2017. He is currently pursuing the Ph.D. degree in electrical and computer engineering with Texas A&M University, TX, USA. His research interests include power system cyber-physical modeling, data-driven power system control, and sparse matrix ordering.

Astrid Layton received her BS in Mechanical Engineering from the University of Pittsburgh in Pittsburgh, PA in 2009 and her Ph.D. in Mechanical Engineering from Georgia Institute of Technology in Atlanta, Georgia in 2014, respectively. She is currently an Assistant Professor at Texas A&M University in the Mechanical Engineering department. Her research looks at bio-inspired network design problems, focusing on the use of biological ecosystems as inspiration for the design of sustainable and resilient complex human networks and systems.

Katherine R.Davis (Senior Member, IEEE) received the B.S. degree from The University of Texas at Austin, Austin, TX, USA, in 2007, and the M.S. and Ph.D. degrees from the University of Illinois at Urbana–Champaign, Champaign, IL, USA, in 2009 and 2011, respectively, all in electrical engineering. She is currently an Assistant Professor of electrical and computer engineering with Texas A&M University. Her research interests include Operation and Control of Power Systems, Interactions between Computer Networks and Power Networks, Security-oriented Cyber-physical Analysis Techniques, Data-driven and Model-based Coupled Infrastructure Analysis and Simulation.